Bulletin of Mathematical Biology
https://doi.org/10.1007/s11538-019-00664-3

Society for Mathematical Biology

ORIGINAL PAPER

Modelling the Host Immune Response to Mature and Immature Dengue Viruses

Milen Borisov[1] · **Gabriel Dimitriu**[2] · **Peter Rashkov**[1]

Received: 15 February 2019 / Accepted: 8 September 2019

Abstract

Immature dengue virions contained in patient blood samples are essentially not infectious because the uncleaved surface protein prM renders them incompetent for membrane fusion. However, the immature virions regain full infectivity when they interact with anti-prM antibodies, and once opsonised virion fusion into Fc receptor-expressing cells is facilitated. We propose a within-host mathematical model for the immune response which takes into account the dichotomy between mature infectious and immature noninfectious dengue virions. The model accounts for experimental observations on the different interactions of plasmacytoid dendritic cells with infected cells producing virions with different infectivity. We compute the basic reproduction number as a function of the proportion of infected cells producing noninfectious virions and use numerical simulations to compare the host's immune response in a primary and a secondary dengue infections. The results can be placed in the immunoregulatory framework with plasmacytoid dendritic cells serving as a bridge between the innate and adaptive immune response, and pose questions for potential experimental work to validate hypothesis about the evolutionary context whereby the virus strives to maximise its chance for transmission from the human host to the mosquito vector.

Keywords Dengue · Mathematical model · Viral dynamics · Immune response

Mathematics Subject Classification 34A34 · 92B05 · 49Q12

Milen Borisov is partially supported by the National Scientific Program *Information and Communication Technologies for a Single Digital Market in Science, Education and Security (IKTvNOS)*, Contract No DO1-205/23.11.2018, financed by the Ministry of Education and Science in Bulgaria. Peter Rashkov acknowledges partial support from the Bulgarian Fund for Scientific Research (FNI) under Contract DKOST01/29.

Electronic supplementary material The online version of this article (https://doi.org/10.1007/s11538-019-00664-3) contains supplementary material, which is available to authorized users.

✉ Peter Rashkov
p.rashkov@math.bas.bg

Extended author information available on the last page of the article

Published online: 20 September 2019

1 Introduction

Multiple vector-borne diseases are caused by flaviviruses (Pierson and Diamond 2012). Flavivirus synthesis in the infected cells requires cleavage of the viral surface protein prM to M by the cellular enzyme furin before the secretion of mature virions from the cell (Zybert et al. 2008). This process, however, appears to be inefficient for the dengue virus (DENV) because sera from DENV patients demonstrate a high proportion of immature virions containing uncleaved prM (Anderson et al. 1997; Bray and Lai 1991). The immature prM-containing DENV particles are essentially not infectious to cells (Zybert et al. 2008) because uncleaved prM renders them incompetent for membrane fusion (Heinz et al. 1994). However, the immature virions regain full infectivity upon interaction with anti-prM antibodies, which facilitate fusion with Fc receptor-expressing cells (Rodenhuis-Zybert et al. 2010). The anti-prM antibodies are weakly to moderately neutralising (Beltramello et al. 2010; Dejnirattisai et al. 2010; Pierson and Diamond 2012) and may play a role in the phenomenon of antibody-dependent enhancement (ADE), a mechanism proposed to explain the more severe form of the disease in a secondary infection caused by a different DENV serotype.

We propose and study a *within-host* model for DENV incorporating the dichotomy between mature versus immature virions. In particular, we focus on the role of plasmacytoid dendritic cells (pDCs), important sentinels in an infection. pDCs sense invading pathogens and can release type I interferon up to thousand-fold times more than other cell types (Wang et al. 2018). This anti-viral compound triggers maturation and activation of the pDCs (Asselin-Paturel et al. 2005; Fitzgerald-Bocarsly et al. 2008; Montoya et al. 2002), activation of NK cells (Wang et al. 2018), and recruitment of other immune cells to the site of infection (McKenna et al. 2005). Mature pDCs also trigger effector and cytotoxic T cells, and they are considered to be an important mediator between innate and adaptive immunity (Mathan et al. 2013; McKenna et al. 2005).

In vitro experiments indicate DENV-infected cells that release immature DENV cause pDCs to produce much higher amounts of interferon in a process mediated by cell–cell contact. The amounts of interferon in this case are higher than in the case of pDCs sensing those cells releasing mature DENV (Décembre et al. 2014; Webster et al. 2018).

The proposed *within-host* model is compartmental involving target cells, infected cells, free virus and different types of immune cells, and anti-viral compounds. The experimentally observed infectious potential of immature virions in the presence of anti-prM antibodies has not been considered in previous within-host DENV models (Ansari and Hesaaraki 2012; Ben-Shachar and Koelle 2015; Ben-Shachar et al. 2016; Clapham et al. 2014; Gujarati and Ambika 2014; Nikin-Beers and Ciupe 2015; Nuraini et al. 2009). We include the degree of maturity and infectivity by including compartments for infectious and noninfectious DENV.

Due to the large number of model parameters with unidentified or uncertain values, the model simulations are based on using random sampling of parameters and Latin hypercube sampling in order to establish relationships between important characteristics of the viral dynamics and immune response. We also perform a global sensitivity analysis to explore the parameter sensitivity in the model. The pDC response is related to various infection parameters such as peak viremia, the time to peak viremia, number

of infected cells and numbers of activated immune cells in a primary and secondary infection.

In particular, we address the issue of disease severity as measured by total viral load and number of infected cells. As ADE is observed in secondary infections with a different DENV serotype or in primary infections of infants of dengue-immune mothers, it has been suggested that already present anti-prM antibody may interfere with immature DENV, increasing the pool of infectious particles and raising the number of infected cells and viremia (Rodenhuis-Zybert et al. 2010)

Furthermore, we use the model to evaluate whether immature DENV has a significant contribution to the disease progression by causing a stronger innate immune response, such as subsequent recruitment of DENV permissive cells vie interferon signalling which increases the pool of target cells, and may lead to a more severe illness (dengue haemorrhagic fever, DHF). The model allows us to investigate the trade-off between production of infectious against noninfectious viral progeny virions; the eco-evolutionary motivation seems unclear, why would the virus benefit from noninfectious virions which induce a stronger interferon response targeted against the virus in general (Décembre et al. 2014).

We study the role of pDCs in light of clinical observations of correlation with the disease outcome of DENV-infected patients (Pichyangkul et al. 2003), and in the context of immune homeostasis during viral infections (Webster et al. 2018). The model predicts that lower prevalence of pDCs is associated with a higher peak count of T cells, which could cause a surge in pro-inflammatory cytokines and characteristic of DHF.

We also place the model into the context of DENV reinfections with the same serotype (Waggoner et al. 2016). We compute and compare the basic reproduction number R_0 in a primary and secondary DENV infection, and discuss how changes in parameter values could shed insight onto the recurrence of disease.

1.1 Description of the Model

We propose a compartmental model for the within-host DENV infection and the immune response for a primary and secondary dengue infection. In the following, a primary infection refers to hosts which have never suffered from dengue, and a secondary refers to hosts which have had a previous dengue infection (possibly asymptomatic).

The model will not consider processes on a longer time scale, such as target or immune cell regeneration (lifespan of macrophages is much larger than the course of a dengue infection) except that of plasmacytoid dendritic cells, or onset of immunological memory (development of antibodies) after a primary infection.

In vitro work has revealed an inverse relation between the level of furin expression in DENV permissive cells, the level of maturity of virions they release, and the pDCs response triggered (production of interferon and inflammatory cytokine). Décembre et al. (2014), Webster et al. (2018), Zybert et al. (2008). Inhibition of furin causes reduction in DENV maturation, and furthermore, cells releasing immature DENV cause pDCs to produce more interferon than cells producing mature virus in co-culture (Décembre et al. 2014, Fig. 9). Due to lack of in vivo data on differences of

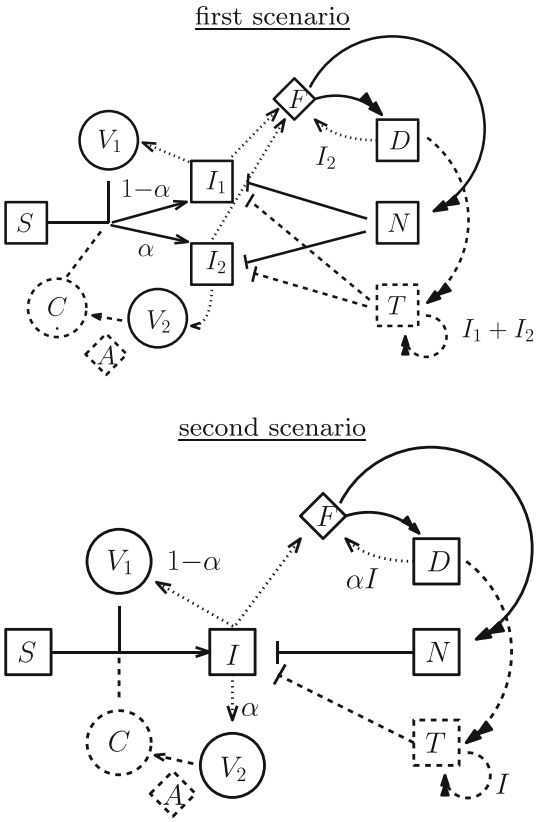

Fig. 1 A cartoon scheme of the two scenarios considered in this work. Here, S denotes target cells, D pDCs, N NK cells, T T cells, F interferon, A anti-prM antibody, V_1 infectious DENV, V_2 noninfectious DENV, C–antibody-V_2 complexes that are not cleared by the immune response and are fully infectious (Rodenhuis-Zybert et al. 2011). A dotted arrow means "production of", a double arrow "activation of/by". Dashed arrows and compartments refer to those compartments present in the models for secondary infection

furin expression among DENV permissive cells or single-cell data on virion release, we propose two scenarios for including this heterogeneity in the model. The first includes modelling two distinct subpopulations of infected cells: I_1 producing mature, infectious DENV and I_2 producing immature, noninfectious DENV that elicit pDC response with different intensities. The second scenario includes just one population of infected cells I, which release both mature and immature virions, and a fraction of the infected cells contributes to increased interferon production by pDCs. The two scenarios are presented in Fig. 1.

In the *first scenario*, the temporal dynamics of the infection and immune response is described as follows. The free mature virus V_1 in a *primary infection* infects target cells S at rate β and both mature and immature virions decay at rate d_V (2d), (2e). In a *secondary infection*, a fraction of the immature DENV particles V_2 opsonises with the anti-prM nonneutralizing antibody A, and forms a complex C at rate k_{a2} (3f). A fraction σ of the complexes escapes clearance by phagocytosis, remains in the body, is able to infect Fc receptor-expressing target cells at rate β and decays at rate d_V (3f). (The increased spectrum of particles able to infect $V_1 + C$ is the so-called antibody-dependent enhancement or ADE) (Rodenhuis-Zybert et al. 2010.)

Note that we may include opsonisation of mature DENV particles with anti-prM antibody as fully or nearly fully infectious DENV could contain small amounts of prM protein, but for the sake of simplicity, in case of a secondary DENV infection with a different serotype, we assume $k_{a1} = 0$. We also neglect for the sake of simplicity dissociation of the virus-antibody complexes.

Target cells S (monocytes, macrophages, etc.,) in a *primary infection* are infected by V_1 (2a) at rate β, and by V_1+C in a secondary infection (3a) but are replenished through recruitment of additional DENV permissive cells (e.g. dendritic cells, T cells Silveira et al. 2018) through the action of interferon (Tough 2012) at a rate γ_S, whose value is varied in the numerical simulations. A fraction α of the infected cells transitions to compartment I_2 producing noninfectious, immature DENV V_2 at per cell rate p, while the remaining transition to compartment I_1 producing mature, infectious DENV V_1 at the same rate. Both types of infected cells are removed by the action of NK cells at rate k_N.

Based on reports the prevalence of the innate over the adaptive immune response for the clearance of the primary infection (Friberg et al. 2011), we assume the role of antibody to be negligible in a primary infection. The innate immune response in a *primary infection* includes only pDC and NK cell response and changes in interferon levels. Infected cells produce interferon F at rate q_2 which decays at rate d_F (2f), (3g). In vitro experiments show cells releasing immature DENV cause pDCs to produce more interferon than cells producing mature virus due to cell–cell contact (Décembre et al. 2014). Hence, we include an additional production term of interferon by pDCs coming into contact with those infected cells producing immature DENV I_2 at rate q_1. The rate q_1 is found by fitting data from in vitro measurements (see Supplementary Material). pDCs D are stimulated by interferon (Asselin-Paturel et al. 2005; Fitzgerald-Bocarsly et al. 2008; Montoya et al. 2002), modelled by the functional response $\Gamma_D(F)$ and are removed at rate d_D (2g).

We shall consider the following type of functional response

$$\Gamma_D(F) = D_0 + \frac{K_D F}{\kappa_F + F} \,. \tag{1}$$

The constant D_0 corresponds to pDC production, while the other summand is the stimulation by interferon F, a Michaelis–Menten term with maximal rate K_D and Michaelis constant κ_F, and assures that pDC levels do not rise rapidly during a dengue infection. (Note pDC levels in dengue fever reported by Pichyangkul et al. (2003) do not exceed a 30% increase than pDC levels in healthy individuals.)

Finally, NK cells N are stimulated by interferon at rate γ_N (Ben-Shachar and Koelle 2015) and are removed at rate d_N (2h).

In summary, the equations describing the primary infection are

$$S' = -\beta S V_1 + \gamma_S F \tag{2a}$$
$$I_1' = (1-\alpha)\beta S V_1 - k_N I_1 N \tag{2b}$$
$$I_2' = \alpha\beta S V_1 - k_N I_2 N \tag{2c}$$
$$V_1' = p I_1 - \beta V_1 S - d_V V_1 \tag{2d}$$

$$V_2' = pI_2 - d_V V_2 \tag{2e}$$
$$F' = q_1 DI_2 + q_2(I_1 + I_2) - d_F F \tag{2f}$$
$$D' = \Gamma_D(F) - d_D D \tag{2g}$$
$$N' = \gamma_N F - d_N N\ . \tag{2h}$$

In a *secondary infection*, we include immunological memory (anti-prM antibodies present in the body A), and cytotoxic T cells T due to their stronger presence in the clearance of a secondary infection (Friberg et al. 2011). The equations describing the secondary infection are

$$S' = -\beta SV_1 - \beta SC + \gamma_S F \tag{3a}$$
$$I_1' = (1-\alpha)\beta S(V_1 + C) - k_N I_1 N - k_T I_1 T \tag{3b}$$
$$I_2' = \alpha\beta S(V_1 + C) - k_N I_2 N - k_T I_2 T \tag{3c}$$
$$V_1' = pI_1 - \beta V_1 S - d_V V_1 - k_{a1} A V_1 \tag{3d}$$
$$V_2' = pI_2 - d_V V_2 - k_{a2} A V_2 \tag{3e}$$
$$C' = \sigma k_{a2} A V_2 - \beta CS - d_V C \tag{3f}$$
$$F' = q_1 DI_2 + q_2(I_1 + I_2) - d_F F \tag{3g}$$
$$D' = \Gamma_D(F) - d_D D \tag{3h}$$
$$N' = \gamma_N F - d_N N \tag{3i}$$
$$T' = \gamma_{T1} T(I_1 + I_2) + \gamma_{T2} T D - d_T T \tag{3j}$$
$$A' = rA\left(1 - \frac{A}{K_a + m(V_1 + V_2)}\right) - k_{a1} A V_1 - k_{a2} A V_2\ . \tag{3k}$$

T cells are activated through cell-to-cell contact with the infected cells at rate γ_{T1} and with pDCs (McKenna et al. 2005) at rate γ_{T2} (3j). Anti-prM antibodies follow a logistic growth law with carrying capacity, dependent on the viral load $V_1 + V_2$ to account for pathogen-stimulated antibody production in a subsequent DENV infection, characterised by immune memory elasticity m in (3k), a lump parameter describing the responsiveness of adaptive immunity. The denominator of (3k) also includes free mature DENV V_1 in order to account for extracellular prM peptides formed during release of such virions that stimulate immunological memory (Rodenhuis-Zybert et al. 2011). Thus, while we do not consider antigen-presenting cells or memory B cells explicitly in our model, it is capable of reproducing a transient increase in antibody production during a subsequent DENV infection before a return to the long-term homeostatic level K_a after the virus has been cleared.

The *per cell* virus production rate p in a secondary infection is kept equal to that of the primary infection. Evidence about the effect of antibodies that facilitate DENV entry into Fc receptor-bearing cells on the number of virion particles produced per cell is not conclusive; some studies report a higher total viral load in a secondary infection (Halstead and O'Rourke 1977), or suggest p is not affected by antibody-mediated entry of immature DENV particles (Rodenhuis-Zybert et al. 2010). However, as experimentally derived, values for p were not available, we use the same p in both (2)

and (3), and assume that the antibody-immature DENV complexes retain the level of infectiousness of the mature, fully infectious DENV.

In the *second scenario* for the within-host response, we consider just one type of infected cells present—the I compartment, which we obtain by adding the equations for I_1, I_2 (see the bottom cartoon in Fig. 1). In a primary infection, thus we have

$$I' = \beta S V_1 - k_N I N, \tag{4}$$

and in a secondary infection,

$$I' = \beta S(V_1 + C) - k_N I N - k_T I T. \tag{5}$$

In this scenario α denotes the fraction of virus produced by the infected cells that is noninfectious, and $1 - \alpha$ the fraction of virus produced by the infected cells that is infectious. The equations for the virus dynamics in a primary infection (2d), (2e) take the form

$$V_1' = p(1-\alpha)I - \beta V_1 S - d_V V_1 \tag{6}$$
$$V_2' = p\alpha I - d_V V_2 \,, \tag{7}$$

and in a secondary infection

$$V_1' = p(1-\alpha)I - \beta V_1 S - d_V V_1 - k_{a1} A V_1 \tag{8}$$
$$V_2' = p\alpha I - d_V V_2 - k_{a2} A V_2 \,. \tag{9}$$

The equation for interferon reads

$$F' = (q_1 \alpha D + q_2) I - d_F F \,, \tag{10}$$

so to account for the cell-to-cell contact-dependent activation of pDCs by DENV-infected cells that produce noninfectious DENV (Webster et al. 2018). The equation for the T cells becomes

$$T' = \gamma_{T1} T I + \gamma_{T2} T D - d_T T \,. \tag{11}$$

Results from the *second scenario* are presented in detail in Section B of the Supplementary Material.

2 Results

We establish some analytical results such as calculation of the basic reproduction numbers R_0 for a primary and secondary infection, and proofs of positivity and boundedness for the solutions of models (2), (3) subject to initial conditions listed in Table 1.

We also show that the ratio between infectious and noninfectious free DENV V_1/V_2 in the model for primary infection converges asymptotically to a steady state. Hence,

Table 1 Initial conditions for the models of a primary (2) and secondary infections (3)

Initial condition	Symbol	Value		Unit	References
		Primary	Secondary		
Number of target cells	$S(0)$	$4 \cdot 10^5$	$4 \cdot 10^5$	cells/ml	Nikin-Beers and Ciupe (2015)
Number of pDC	$D(0)$	D_0/d_D	D_0/d_D	cells/ml	
Number of NK cells	$N(0)$	10^{-6}	10^{-6}	cells/ml	–
Number of T cells	$T(0)$	–	10^3	cells/ml	Ben-Shachar and Koelle (2015)
Mature virions	$V_1(0)$	10	10	copies/ml	–
Immature virions	$V_2(0)$	10	10	copies/ml	–
Opsonised immature virions	$C(0)$	–	0	copies/ml	
Infected cells	$I_{1,2}(0)$	1	1	cell/ml	
Interferon	$F(0)$	0	0	pg/ml	
Antibodies	$A(0)$		K_a	copies/ml	

the parameter α can be related to experimental data about the fraction of such virions in patient blood samples. In fact, numerical simulations show that the asymptotic estimate is reached during the viral growth phase. A similar asymptotic estimate can be established in a secondary infection, except that we must count the noninfectious DENV opsonised with antibody C, and assume $\sigma \approx 1$. Details are given in the Supplementary Material.

We carry out numerical simulations for different parameter values in order to account for uncertainty in parameters and different scenarios of abundance of infected cells producing mature or immature DENV (as given by α). The numerical simulations have been done in the programming language `Python`.

2.1 Basic Reproduction Number in a Primary Versus Secondary Infections

The model is target cell limited, and hence the unique equilibria are disease-free equilibria given by hyperplanes. If we neglect the clearance of NK cells during the window of infection ($d_N = 0$), we have the disease-free equilibrium

$$E^p = (S_0, 0, 0, 0, 0, 0, D_0/d_D, N_0)$$

for the model of primary infection (2), and

$$E^s = (S_0, 0, 0, 0, 0, 0, 0, D_0/d_D, N_0, 0, K_a)$$

for the secondary infection (3). In the secondary infection, the equilibrium corresponding to $A = 0$ is locally unstable and not relevant for our analysis.

The basic reproduction number shows the average number of infected cells generated from one virus in a fully susceptible population. Using the next-generation matrix (van den Driessche and Watmough 2002) (see details in the Supplementary Material), we find an exact expression for the basic reproduction number in a primary infection,

$$\mathcal{R}_0^p = \sqrt{\frac{(1-\alpha)p\beta S_0}{k_N N_0 (d_V + \beta S_0)}}. \tag{12}$$

For a secondary infection, we obtain an approximation

$$\mathcal{R}_0^s \approx \sqrt{\frac{p}{k_N N_0} \frac{(1-\alpha)\beta S_0}{\beta S_0 + k_{a1} K_a + d_V}} + \frac{3}{2} \cdot \frac{\sigma k_{a2} K_a}{k_{a2} K_a + d_V} \frac{\alpha(\beta S_0 + k_{a1} K_a + d_V)}{(1-\alpha)(\beta S_0 + d_V)}. \tag{13}$$

This estimate gives us an opportunity to evaluate and compare $\mathcal{R}_0^s$ in a scenario of a secondary infection with a different or identical DENV serotype. For a different serotype $k_{a1} = 0$ because pre-existing, nonneutralizing prM antibody would not opsonise with the infectious DENV particles. Then, (12) implies $\mathcal{R}_0^p = \sqrt{P}$, and (13) simplifies to

$$\mathcal{R}_0^s \approx \mathcal{R}_0^p + \frac{3}{2} \cdot \frac{\sigma k_{a2} K_a}{k_{a2} K_a + d_V} \cdot \frac{\alpha}{1-\alpha}.$$

Due to the presence of anti-prM antibody $K_a > 0$, $\mathcal{R}_0^s > \mathcal{R}_0^p$ holds, so the basic reproduction number in this scenario would exceed that in a primary infection.

In a secondary infection with the same DENV serotype, most studies report lack of viremia. Thus, the basic reproduction number $\mathcal{R}_0^s$ would be expected to be less than 1 or at least such that viral loads are below the detection threshold. Judging from the estimate (13), in order to reduce the value of $\mathcal{R}_0^s$ significantly below $\mathcal{R}_0^p$ (or below 1), one would have several options: to reduce the infectivity rate β, increase the binding rate of anti-prM antibody to infectious DENV particles k_{a1}, the viral clearance rate d_V, the kill rate of NK cells k_N, or reduce the proportion σ of opsonised noninfectious DENV that is able to infect target cells. The last option can be interpreted as improving the clearance of such immune complexes by phagocytosis or other means.

2.2 Numerical Simulations

The proposed model contains many parameters whose values are uncertain or non-identifiable, so it can be at best used to assess qualitative behaviours. In order to examine the behaviour of solutions and to account for the uncertainty, we perform random sampling of model parameters and run multiple simulations. The course of a primary versus secondary infection for a sample set of parameter value (listed in Tables C.1, C.2 in the Supplementary Material) is shown in Fig. 2, and these agree qualitatively with the DENV infection characteristics.

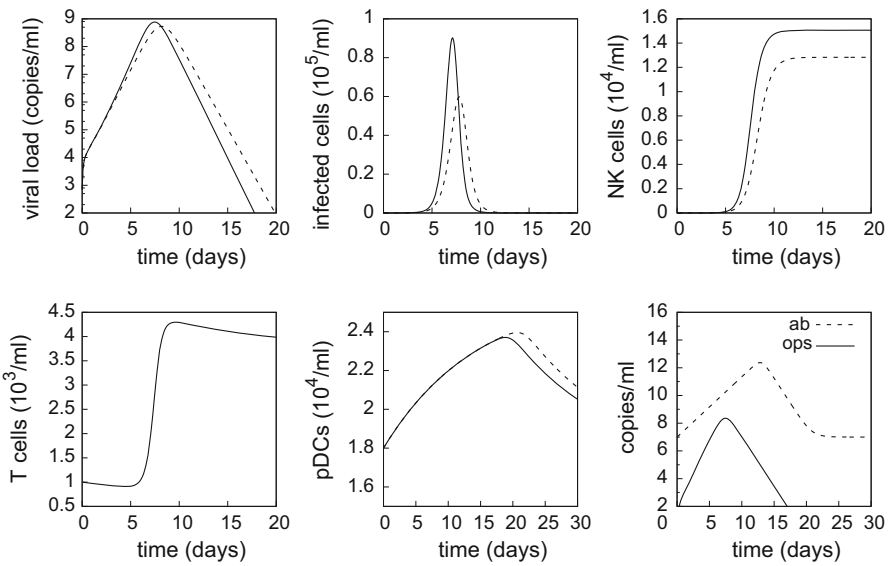

Fig. 2 Time plots of temporal dynamics in a primary DENV infection (dashed lines) and secondary DENV infection (solid lines). The panels show (*clockwise*): viral loads ($V_1 + V_2$ in a primary, resp. $V_1 + V_2 + C$ in a secondary infection), number of infected cells $I_1 + I_2$, NK cells, T cells, pDCs, anti-prM antibody (ab) and opsonised immature DENV (ops) in the secondary infection

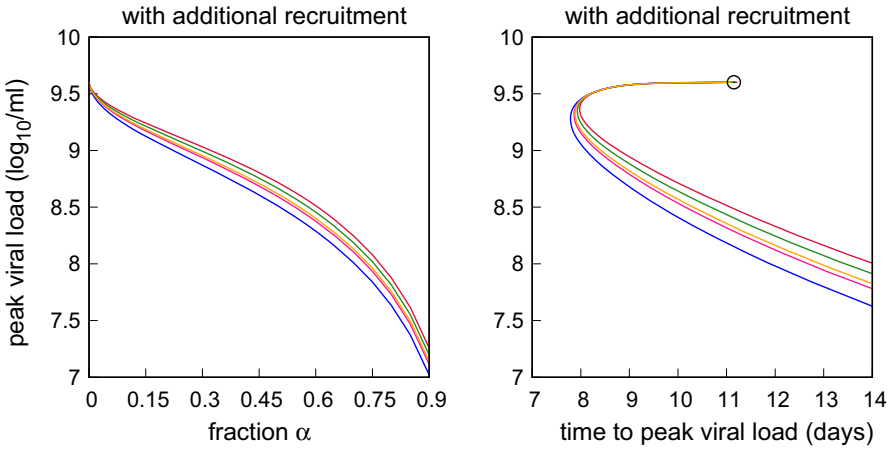

Fig. 3 Relationship between the fraction of infected cells producing immature noninfectious DENV particles α, time to peak viral load, peak viral load for a primary infection. Each series corresponds to a set of parameters k_N, k_F, γ_N, q_1 that are taken from a uniform distribution with range $\pm 15\%$ of the values shown in Table C.1 in the Supplementary Material. The fraction α is in the range [0, 0.9]. The circle in each panel represents the combination at $\alpha = 0$ (Color Figure Online)

To gain understanding of the effect of the parameter α, describing the fraction of infected cells producing immature noninfectious virions, on the disease indicators and immune response, we carry numerical simulations based on Latin hypercube sampling (Marino et al. 2008).

As disease indicators, we take the peak viral load (for the primary infection PVL $= \max_t V_1(t) + V_2(t)$, and for the secondary PVL $= \max_t V_1(t) + V_2(t) + C(t)$), the maximal number of infected cells $MI = \max_t I_1(t) + I_2(t)$ in the first scenario and $MI = \max_t I(t)$ in the second scenario, and the time of peak viral load taking as reference at $t = 0$ the moment when the viral load equals the limit of detection of 357 copies/ml (Nikin-Beers and Ciupe 2015) because of lack of clear evidence for the viral load where dengue fever patients manifest symptoms. For the immune response indicators, we take the peak levels of NK cells, interferon, T cells, and antibodies from the generated time series in the model solutions.

We perform simulations of the primary infection model (2) where we randomly sample the parameters k_N, k_F, γ_N, q_1 from a uniform distribution. The distribution range is $\pm 15\%$ of the respective value shown in Table C.1 in the Supplementary Material. For each sample set, we vary α in the range [0, 0.9) and record the respective maximal value. Results of these simulations are shown in Fig. 3.

As a further step, we simulate the effect of varying α in a primary and a secondary infections. For the set of parameter values shown in Table C.2 in the Supplementary Material, we vary α in the range [0, 0.9) and record the respective maximal value. We consider also the scenario where only a fraction of the opsonised noninfectious DENV may enter Fc receptor-bearing cells ($\sigma = 0.75$) and the scenario where additional target cells can be recruited due to the action of interferon signalling $\gamma_S > 0$. The results are plotted in Figs. 4, 5, and 6.

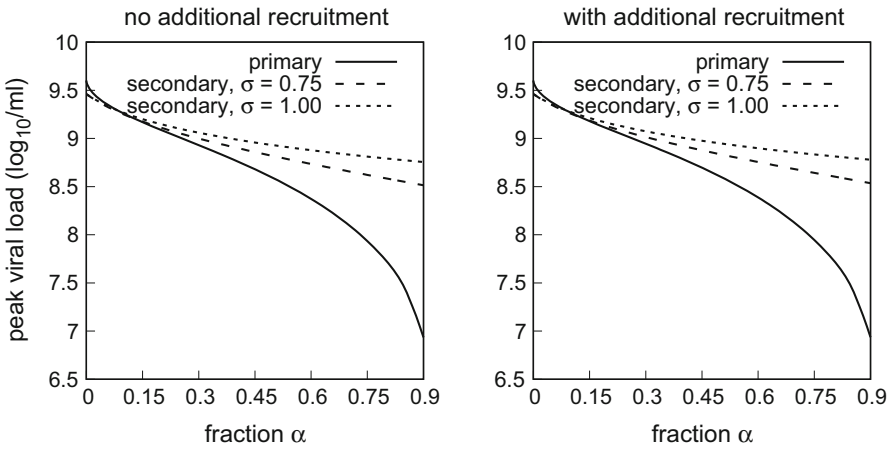

Fig. 4 Relationship between the fraction of infected cells producing immature noninfectious DENV α and the peak viral load in a primary versus secondary infection. For the secondary infection, we consider two values of the fraction σ of opsonised immature particles becoming infectious as indicated. In the left panel, we assume no additional recruitment of target cells ($\gamma_S = 0$), while in the right panel, there is additional recruitment ($\gamma_S = 0.0005$)

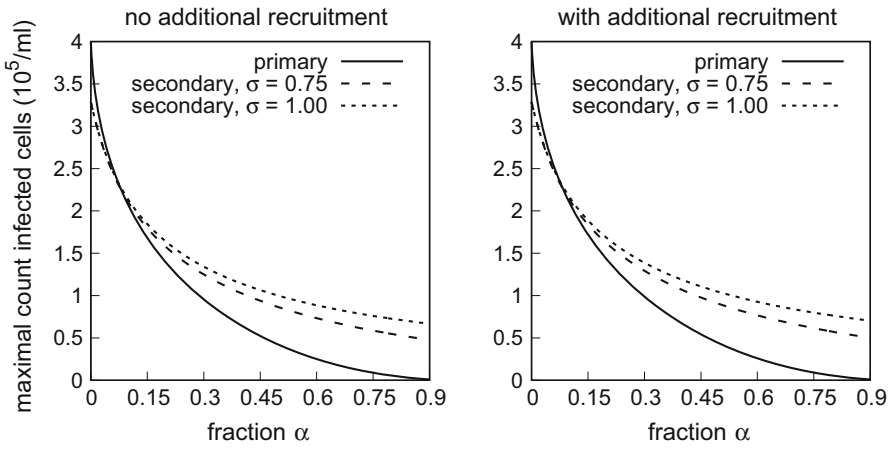

Fig. 5 Relationship between the fraction of infected cells producing immature noninfectious DENV α and the maximal amount of infected cells in a primary versus secondary infection. For the secondary infection, we consider two values of the fraction σ of opsonised immature particles becoming infectious as indicated. In the left, we assume no additional recruitment of target cells ($\gamma_S = 0$) due to interferon signalling, while in the right, there is additional recruitment ($\gamma_S = 0.0005$)

As a second test, we perform a Latin hypercube sampling, that is, we sample randomly $k_N, k_T, k_F, \gamma_N, \gamma_{T1}, \gamma_{T2}, k_{a2}, q_1$ from a uniform distribution with range $\pm 15\%$ of the value shown in Table C.1, C.2 in the Supplementary Material. This value of $\alpha = 0.35$ corresponds to the share of immature DENV found in patient sera (Rodenhuis-Zybert et al. 2010). The values of D_0 vary in the same distribution with

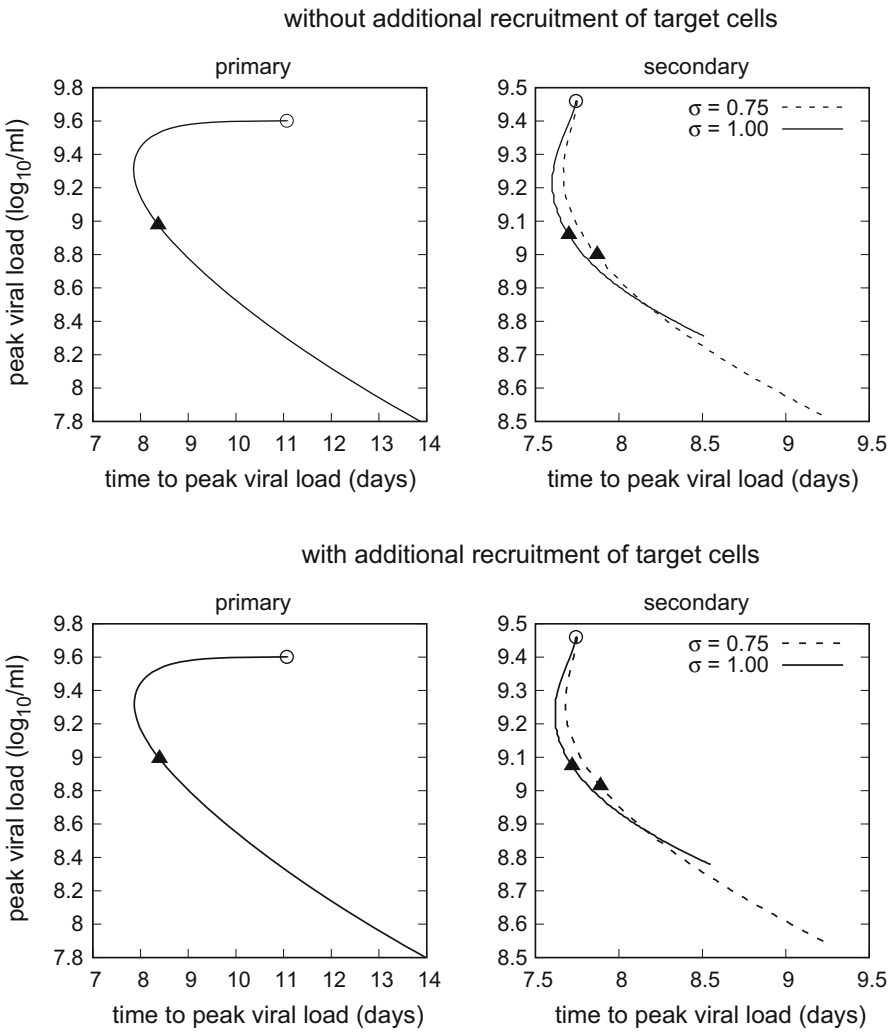

Fig. 6 Relationship between time of maximal viral load and maximal viral load for the fraction of infected cells producing immature noninfectious virions $\alpha \in [0, 0.9]$ for a primary infection (*left panel*) and secondary infection (*right panel*). The value $\alpha = 0$ is shown as an empty circle, and the value $\alpha = 0.3$ is shown as a solid triangle. We consider both no additional recruitment of target cells $\gamma_S = 0$ (top panels) and recruitment of target cells due to interferon signalling ($\gamma_S = 0.0005$) (bottom panels). The fraction of opsonised immature particles becoming infectious in a secondary infection σ as indicated

mean 1250 cell/ml, which corresponds to the pDC production rate reported by Chen et al. (2013).

We compare the times to peak viral load and peak viral load in a primary versus secondary infections from the generated time series in the simulations. Time is measured from the reference point $t = 0$ where the viral load is at the limit of detection. Since the distribution of the generated times to peak viral load and peak viral load in

Table 2 Comparing the sample distributions of peak viral loads and times to peak viral load in primary versus secondary infections (sample mean and standard deviation (SD)) for two values of σ

	Primary infection		Secondary ($\sigma = 0.75$)			Secondary ($\sigma = 1$)		
	Sample Mean	Sample SD	Sample Mean	Sample SD	p Value	Sample Mean	Sample SD	K–S p value
PVL (10^7)	53.1	6.77	67.6	7.4	$< 10^{-20}$	80.7	8.49	$< 10^{-20}$
Time to PVL	8.55	0.084	7.87	0.061	$< 10^{-20}$	7.68	0.056	$< 10^{-20}$

The values are generated from 100 simulations of the models with randomly sampled values $k_N, k_T, k_F, \gamma_N, \gamma_{T1}, \gamma_{T2}, k_{a2}, q_1, D_0$ from a uniform distribution. Models employed with $d_N = 0$. The p values are taken from a two-sample Kolmogorov–Smirnov test

Table 3 Comparing the sample distributions of peak viral loads in primary versus secondary infections [sample mean and standard deviation (SD)] under assumption of additional target cell recruitment $\gamma_S = 0.0005$ (*columns*)

	$\gamma_S = 0$ Sample Mean	Sample SD	$\gamma_S > 0$ Sample Mean	Sample SD	K–S p Value
Primary	5.31×10^8	6.77×10^7	5.45×10^8	7.09×10^7	0.15
Secondary ($\sigma = 0.75$)	6.76×10^8	7.4×10^7	6.96×10^8	7.74×10^7	0.15
Secondary ($\sigma = 1$)	8.07×10^8	8.49×10^7	8.3×10^8	8.87×10^7	0.15

The values are generated from 100 simulations of the models with randomly sampled values $k_N, k_T, k_F, \gamma_N, \gamma_{T1}, \gamma_{T2}, k_{a2}, q_1, D_0$ from a uniform distribution with range $\pm 15\%$ of the value shown in Table C.1, C.2 in the Supplementary Material. Models employed with $d_N = 0$. The p values are taken from a two-sample Kolmogorov–Smirnov test

the sample is unknown, we use a nonparametric two-sample Kolmogorov–Smirnov (K–S) test (Gibbons and Chakraborti 2010, Section 6.3) to test whether the generated samples of disease indicators from models (2) and (3) come from the same distribution. The null hypothesis of the K–S test is "distributions of disease indicators in primary versus secondary infections are the same". If the peak viral loads generated by models for primary and secondary infections came from the same distribution, then the sampled values would not be statistically significantly different. The mean and standard deviation of the sample peak viral load and sample time to peak viral load in the primary and secondary infections and the p value of the Kolmogorov–Smirnov test are shown in Table 2.

Finally, we use the generated sample time series to check whether the effect of additional recruitment of target cells on the maximal viral load significantly affects the peak viral load. The null hypothesis of the K–S two-sample test is "distribution of peak viral loads in the model without and with additional recruitment of target cells are the same". The mean and standard deviation of the peak viral load in a primary and secondary infections without and with additional recruitment of target cells [$\gamma_S = 0$ vs. $\gamma_S > 0$ in Eqs. (2a) or (3a)] and the p value of the hypothesis test are shown in Table 3.

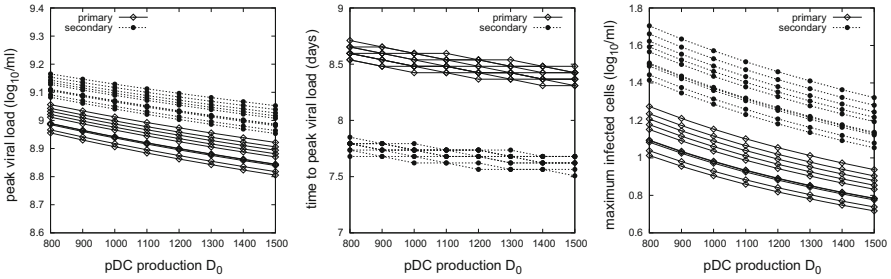

Fig. 7 Relationship between pDC production rate D_0, peak viral load, time to peak viral load and maximal count of infected cells. The parameter $\alpha = 0.35$

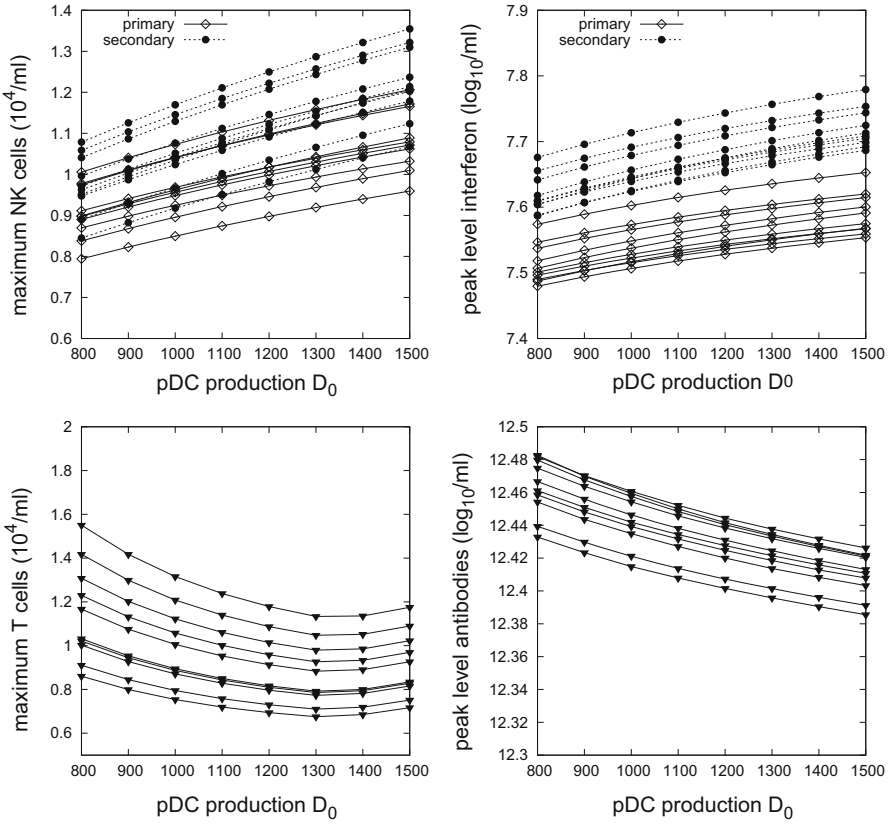

Fig. 8 Relationship between pDC production rate D_0, and the immune response: maximum counts of NK cells and T cells (left panels), peak level of interferon and peak level of antibodies (right panels). The parameter $\alpha = 0.35$

Next, we examine the contribution of the term describing pDC production D_0 in homeostasis for the dynamics of the primary and secondary infections. We randomly sample the parameters describing the immune response to DENV,

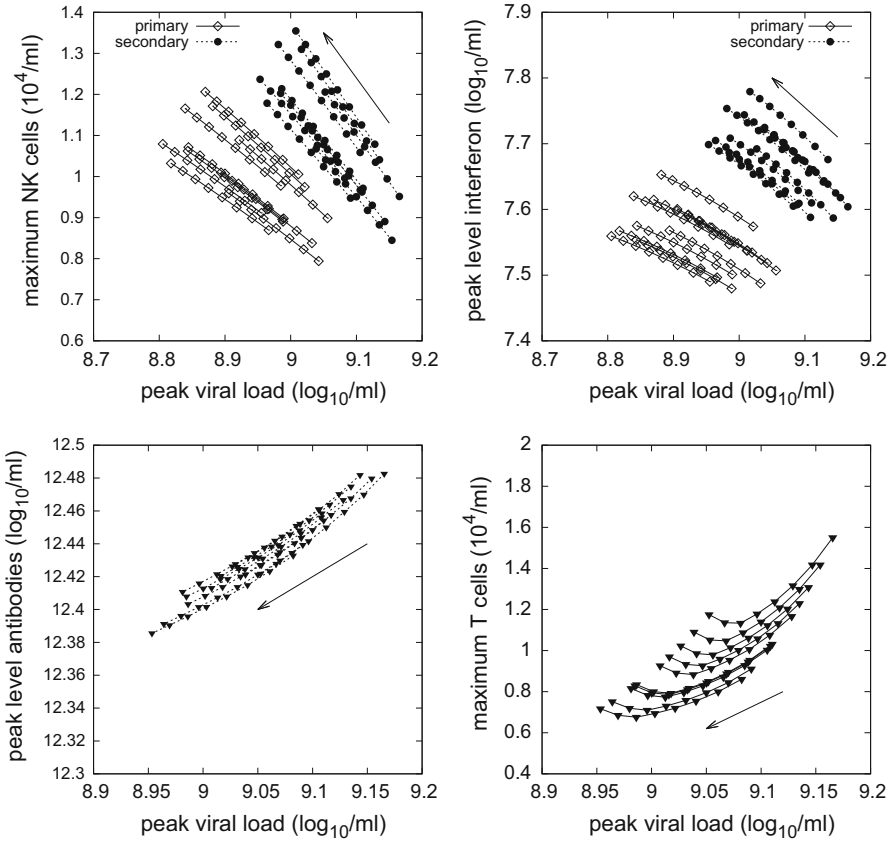

Fig. 9 Relationship between peak viral load, peak level of interferon and peak level of antibodies, maximum counts of NK cells and T cells. The parameter $\alpha = 0.35$. The arrow points in the direction of increasing D_0

$k_N, k_T, k_F, \gamma_N, \gamma_{T1}, \gamma_{T2}, k_{a2}, q_1$, from a uniform distribution with range $\pm 15\%$ of the value shown in Tables C.1, C.2 in the Supplementary Material. For each sample set, we vary D_0 in the range [800, 1500] and record the maximal viral load, maximal number of infected cells, NK cells, T cells, and maximal level of interferon, and anti-prM antibodies. The relationship between D_0 and peak viral load and time to peak viral load is shown in Fig. 7.

The relationship between D_0 and peak number of infected cells, peak numbers of NK and T cells and peak levels of interferon, and antibodies is shown in Fig. 8.

In addition, we plot the combinations between peak viral load, peak number of infected cells, peak antibody level, and maximal numbers of NK and T cells (Fig. 9). In these plots, each series corresponding to a given sample of $k_N, k_T, k_F, \gamma_N, \gamma_{T1}, \gamma_{T2}, k_{a2}, q_1$ is drawn as a curve, with an arrow representing the changes in the respective quantities along the curve with D_0 increasing from 800 to 1500.

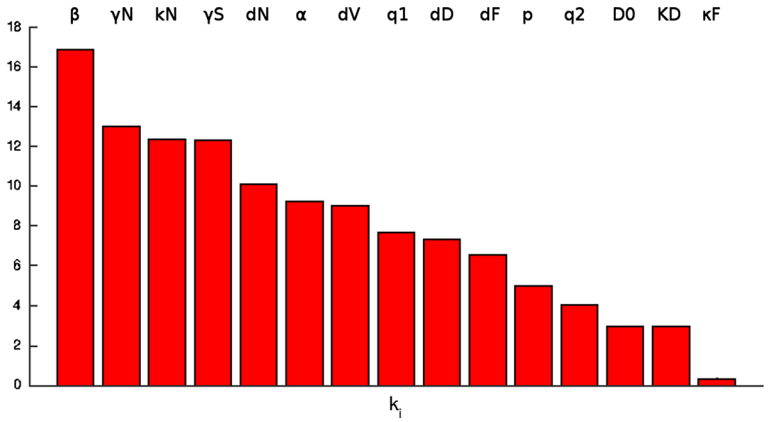

Fig. 10 Parameter sensitivity spectrum illustrating the effect of each parameter with respect to first principal component (*primary infection*) in the first scenario. The parameter β (per virion infection rate) is found the most sensitive among all the model parameters, followed by γ_N (stimulation of NK cells by interferon), κ_N (the removal rate of infected cells by the action of NK cells), and γ_S (recruitment rate of target cells by interferon)

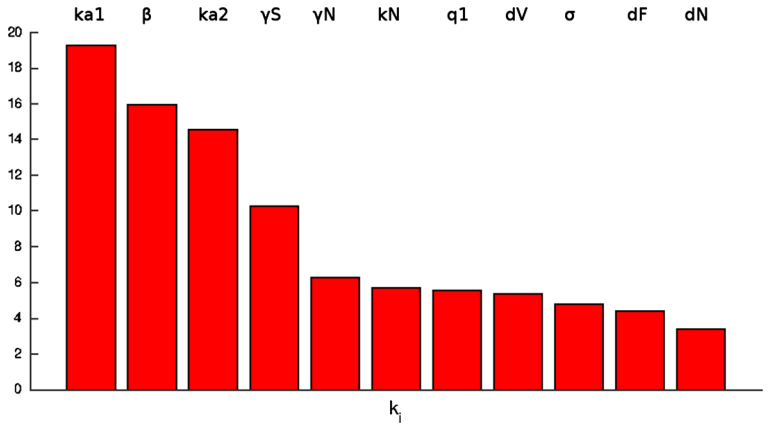

Fig. 11 Parameter sensitivity spectrum depicting the effect of the most significant 11 parameters (among all 25 parameters of the model) with respect to first principal component (*secondary infection*) in the first scenario. The rate k_{a1} (opsonisation of infectious DENV) is the most sensitive among all the model parameters, followed by the infection rate β and k_{a2} (opsonisation of noninfectious DENV)

Finally, we globally analyse the sensitivity of the within-host immune response to mature and immature dengue virus by means of two graphical objects: the sensitivity heat map (see Figs. A.7 and A.9 in the Supplementary Material) and the parameter sensitivity spectrum for both models (2) and (3). Our approach reveals how the solutions change after model parameters are perturbed.

The sensitivity heat maps show the degree of sensitivity of the variables to parameter variation. The parameter sensitivity spectrum, or strength values (Figs. 10 and 11) for the *first scenario*, represents the effect of perturbing each parameter on the time series of the solution.

In the heat map (Fig. A.7 in the Supplementary Material) for the primary infection (2), the variable D (plasmacytoid dendritic cells) presents the highest sensitivity, followed by S (target cells) then N—natural killer cells We also remark that only D exceeds 75% of the global maximum (highlighted by the rectangle in magenta colour in Fig. A.7 in the Supplementary Material). The parameter β (infection rate of target cells by mature DENV) is found to be the most sensitive among all the model parameters, followed by the recruitment rate of natural killer cells by interferon γ_N, and the removal rate of infected cells by the action of NK cells κ_N. The rate of additional recruitment of target cells due to interferon signalling γ_S is in fourth place. In a secondary infection (3), the variable C (antibody-noninfectious DENV complexes) presents the highest sensitivity, followed by F (interferon), V_1 (mature, fully infectious DENV) (Fig. A.9 in the Supplementary Material). That plot indicates that only variable C exceeds 75% of the global maximum (highlighted by the rectangle in magenta colour). The parameter k_{a1} (opsonisation of mature, infectious DENV) is the most sensitive among all the model parameters, followed by β (infection rate of target cells) and k_{a2} (opsonisation of immature, noninfectious DENV).

In the *second scenario*, in the model for primary DENV infection, the variable D (plasmacytoid dendritic cells) presents the highest sensitivity, followed by S (target cells), and then F (interferon). We also remark that only variable D plasmacytoid dendritic cells exceed 95% of the global maximum (highlighted by the rectangle in magenta colour in Fig B.10 of the Supplementary Material). The parameter D_0 (pDC production) is found the most sensitive among all the model parameters, followed by K_D (maximum rate of pDCs recruitment), p (virus production rate), and κ_F, the Michaelis constant in recruitment of pDC (Fig. 12). In the model for secondary DENV infection, the variable C (antibody-noninfectious DENV complexes) presents the highest sensitivity, followed by I (infected cells), V_1 (mature DENV), and then

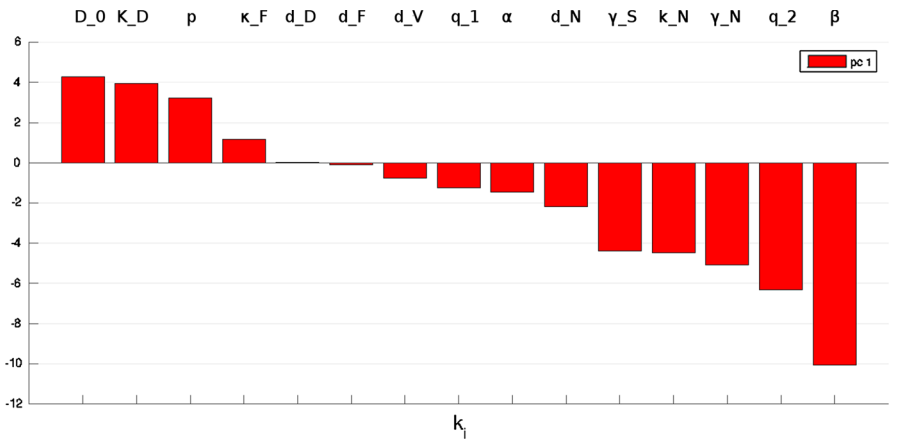

Fig. 12 Parameter sensitivity spectrum illustrating the effect of each parameter with respect to first principal component (primary infection) for the second scenario. The parameter D_0 (pDC production) is found the most sensitive among all the model parameters, followed by K_D (max. recruitment pDCs), p (virus production rate), and κ_F (Michaelis constant, recruitment pDC)—Experiment #1 (Model DENGUE1)

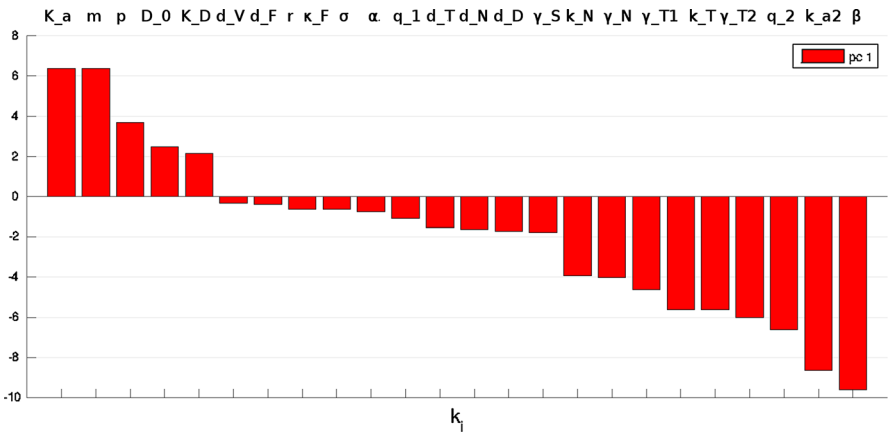

Fig. 13 Parameter sensitivity spectrum depicting the order of the most significant parameters (among all 24 parameters of the model) with respect to first principal component (secondary infection) for the second scenario. The parameter K_a (representing the antibody carrying capacity) is the most sensitive among all the model parameters, followed by m (immune memory elasticity), p (virus production rate), and D_0 (pDC production)

F (interferon) (Figure B.14 in the Supplementary Material). The parameter K_a (representing the antibody carrying capacity) is the most sensitive among all the model parameters, followed by m (immune memory elasticity), p (virus production rate), and D_0 (pDC production) (Fig. 13).

3 Discussion

We have proposed a model incorporating infectious and noninfectious DENV and plasmacytoid dendritic cells to model the within-host immune response based on experimental observations made *in vitro*. Plasmacytoid dendritic cells have different response to DENV-infected cells (Décembre et al. 2014) based on the type of DENV these cells produce.

We study computationally the changes of these characteristics over the course of DENV infection in the host. The model produces signatures of secondary DENV infection: higher peak viremia and shorter times to peak viremia as measured since time of viral load being at limit of detection. We have used a value of $\alpha = 0.35$ close to that reported in the literature (Rodenhuis-Zybert et al. 2010). However, in contrast to other models (e.g. Ben-Shachar and Koelle 2015), our model predicts higher peak viremia in secondary infection with different serotype without assuming a higher infectivity rate for the secondary infection. (We assume β is the same for both primary and secondary infections, see Tables C.1, C.2 in the Supplementary Material).

To verify that this difference between primary and secondary infections is significant, we perform statistical tests on the simulated samples. We have used the Kolmogorov–Smirnov test to test the null hypothesis that the computed samples of peak viral load in a primary and secondary infections come from the same distribution.

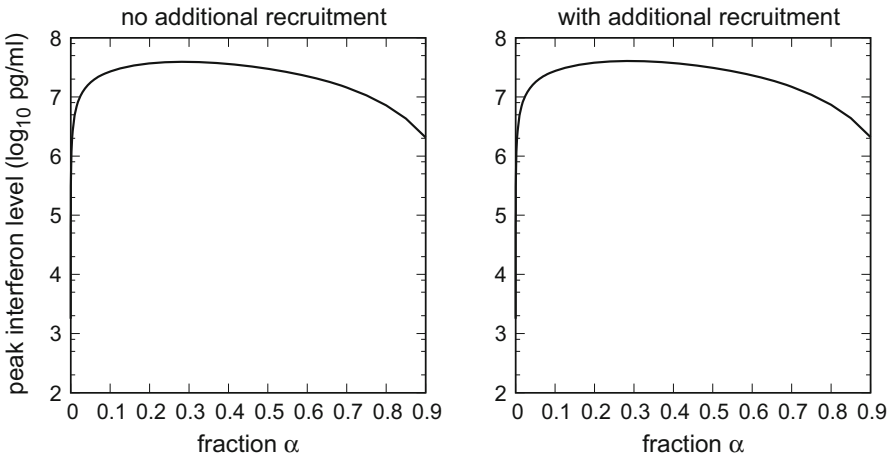

Fig. 14 Relationship between the fraction of infected cells producing immature noninfectious DENV α and the peak level of interferon in the window of infection in a primary infection. In the left, we assume no additional recruitment of target cells ($\gamma_S = 0$) due to interferon signalling, while in the right, there is additional recruitment ($\gamma_S = 0.0005$)

The computed p values from 100 simulated trials are very low (less than 10^{-20}), and allow us to reject the null hypothesis regardless of whether we assume $d_N = 0$ (values in Table 2), or $d_N > 0$ (Table A.2 in the Supplementary Material for the *first scenario* and Table B.1 for the *second scenario*). The hypothesis test also shows that the time to peak viremia in a secondary infection is shorter compared to the primary infection.

The models (2), (3) test the effect of noninfectious particles in DENV infection. The results show the maximal number of infected cells and peak viremia decrease as the share of cells producing noninfectious DENV increases (Figs. 4, 5). For low values $\alpha < 0.1$, the peak viremia level in a primary infection is higher than that in a secondary infection. Otherwise, the peak viremia level in a secondary infection is higher even though the models in both scenarios use the same infection rate per virion β. The literature reports values for α at about 0.3 (Rodenhuis-Zybert et al. 2010), and reported higher peak viral loads in a secondary infection are consistent with the model results for such values of α. The peak levels of interferon as function of α in a primary infection are plotted in Fig. 14: maximum peak level is for intermediate α.

Figures 3 (right panel) and 6 show the combinations of the values of times to peak viral loads and peak viral loads as the parameter α is varied between 0 and 0.9. The relationships are C-shaped in both primary and secondary infections. As the fraction of cells producing noninfectious DENV α increases from 0, both peak viral load and the time to peak viremia decrease. Beyond a threshold value of α, however, the time to peak viral load starts to increase, while the peak viral load continues to drop. In a secondary infection, a similar relationship holds, but the C-curve is "flatter". The C-shaped relationship between the times to peak viral load and peak viremia levels is retained even if we consider NK cell removal, $d_N > 0$ (shown in Fig. A.4 in the Supplementary Material). The same holds for the plots of maximal levels of interferon (Fig. A.3 in the Supplementary Material).

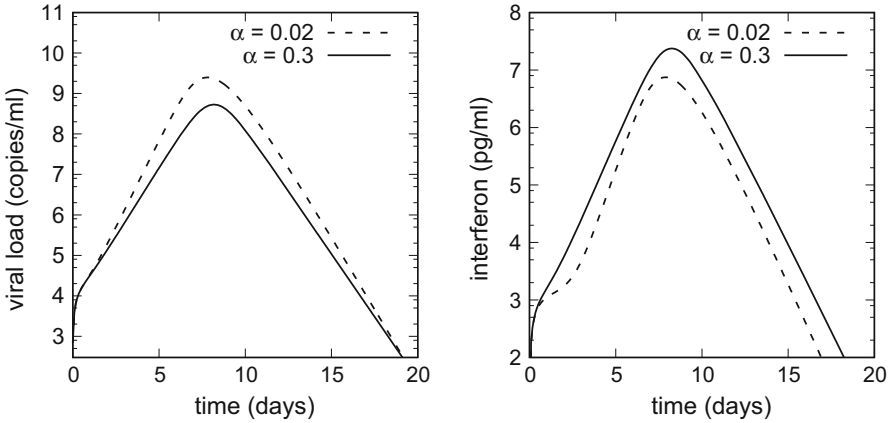

Fig. 15 Comparison between viremia and interferon dynamics for different fractions of cells producing noninfectious DENV (α) in a primary infection (2)

These results reveal a nonlinear *trade-off* between fractions of cells producing noninfectious DENV, peak viremia level, time to peak viremia, and peak interferon levels. From an eco-evolutionary point of view, the virus must maximise the odds of transmission to effectively complete the cycle of spread from host to vector, and to continue its propagation among susceptible individuals in the population. Most cases of dengue fever are self-limiting, and the virus does not persist in the host over an extended time. A reasonable assumption would be that DENV would be more likely to be transmitted from a DENV-infected host to a vector if the viral loads in the host are higher. However, the level of host viremia required for a successful transmission back to the vector is unknown, and neither is any other physiological condition (febrile symptoms, sweating, etc.,) that could predispose an infected host to become an attractive target for mosquitoes to feed on. Such symptoms could be caused, for example, by higher levels of cytokines, such as interferon, whose production in our model is enhanced via pDCs reacting to infected cells producing immature, noninfectious DENV (Fig. 15). Hence, the presence of noninfectious virions might enable the virus to increase its odds of transmission by several instruments: timing and level of peak viremia, as well as causing febrile symptoms in the host through cytokine secretion. Yet, relationships between cytokine levels and physiological symptoms are likely to be nonlinear or difficult to quantify, e.g. in the case of dengue transmission between asymptomatic hosts and vectors (Duong et al. 2015).

In studying, the role of plasmacytoid dendritic cells in a DENV infection and the immune response the model is also consistent with the view that these cells function as mediators between innate and adaptive immunity (McKenna et al. 2005). It predicts a trade-off in the activation of different types of immune cells (natural killer cells versus cytotoxic T cells) in the secondary infection. This is important because T cells contribute more for clearance of infected cells in the secondary infection than the primary DENV infection (Friberg et al. 2011).

A higher pDC production D_0 is associated with a decrease in the peak viral load and peak numbers of infected cells in primary and secondary infections, as well as the time

to peak viremia (Figs. 7, 8). Higher values of D_0 also translate in higher peak numbers of NK cells and higher peak levels of interferon in both primary and secondary DENV infection with a different serotype (Fig. 8). However, in the secondary infection, the relationship between pDC production rate and peak count of T cells, $\max_t T(t)$, is non-monotone, U-shaped (Fig. 8), and there is a range where a lower pDC production rate D_0 corresponds to a higher peak count of activated T cells. This quantitative feature may suggest the presence of a trade-off between pDC production and T cell activation. Over this range, the term TI describing activation of T cells from infected cells in (3j) dominates the term TD describing activation by pDCs. There, are NK cells are not sufficiently activated by interferon that pDCs produce. In short, scarcity of pDCs disrupts their ability to serve as mediators between innate and adaptive immunity.

In the light of available experimental and clinical evidence, we interpret this model prediction as follows. A secondary DENV infection is associated with dengue haemorrhagic fever (DHF) due to pro-inflammatory cytokines which are partly secreted by T cells (Kurane et al. 1994; Dung et al. 2010). Larger numbers of activated T cells are present in DHF cases during the febrile phase than in patients with milder disease (Green et al. 1999; Mathew and Rothman 2008). If we assume a simple proportional relationship between the pro-inflammatory cytokines and the disease severity, and employ a model for cytokine dynamics which is positive monotone-dependent on the numbers of T cells as in [Ben-Shachar and Koelle (2015), Eq. (4.1)], then the model would translate these results into a higher level of pro-inflammatory cytokines and a higher disease severity at lower pDC production rates D_0. In fact, clinical evidence suggests that an insufficient pDC count is associated with higher viral load and severe disease (Pichyangkul et al. 2003). The model presented in this study suggests that a lower pDC level in a secondary infection seems to be compensated by a stronger T cell response resulting in a higher peak viremia and potentially a higher pro-inflammatory cytokine response and agrees with experimental evidence about the importance of pDCs in immune homeostasis (Webster et al. 2018).

Next, we test the hypothesis whether pDC activation by infected cells and production of interferon that may lead to the possible subsequent recruitment of DENV permissive cells (Décembre et al. 2014). In other words, the noninfectious DENV may act as an "interferon bait" attracting additional dendritic cells, T cells, etc., to the infection site (Silveira et al. 2018). We have introduced a parameter γ_S into the equation for DENV target cells to account for a scenario without additional recruitment ($\gamma_S = 0$) and with additional recruitment ($\gamma_S > 0$). The numerical simulations demonstrate that subsequent recruitment of DENV permissive cells due to interferon signalling ($\gamma_S > 0$) does not significantly increase peak viremia. We have used the Kolmogorov–Smirnov test to check if the computed samples of peak viral load with $\gamma_S = 0$ and $\gamma_S > 0$ come from the same distribution (Gibbons and Chakraborti 2010). The computed p value from 100 simulated trials do not allow us to reject the null hypothesis regardless of whether we take $d_N = 0$ (Table 2), or $d_N > 0$ (Table A.3 in the Supplementary Material) at 1% confidence level. Therefore, our computational model cannot serve as qualitative evidence for noninfectious, immature DENV serving as an "interferon bait", and we suggest more experimental effort to be focused on validate this hypothesis experimentally.

Finally, we discuss the implications of the model in the context of the reported disease incidence in DENV reinfections with the same serotype (Waggoner et al. 2016). We have computed the basic reproduction numbers R_0 in a primary infection (12) and made a first-order approximation for the secondary infection (13). The expression for the secondary infection R_0^s shows that the value R_0^s could be lowered by several means: reduced infectivity rate β, increased binding rate of anti-prM antibody to infectious DENV particles k_{a1}, the viral clearance rate d_V, the kill rate of NK cells k_N, or reduced proportion σ of opsonised noninfectious DENV complexes that are not cleared by phagocytosis. The effect of increasing k_{a1} is ambiguous because of the opposing effect on either summand in the approximation (13). Reducing σ to 0 would affect the second summand only. Yet the infectivity rate β can be reduced and the viral clearance rate d_V can be increased due to the presence of neutralising antibodies, such as anti-E antibodies (Costa et al. 2013; Dejnirattisai et al. 2010). If this is not the case, the basic reproduction number in a secondary DENV reinfection with the same serotype could be sufficiently high and even comparable to that of the primary infection.

In the *first scenario* of the model, we have employed a dichotomy by considering the compartment of infected cells to be split into two subpopulations, I_1 consisting of cells producing mature virus, and I_2 of cells producing immature virus. That model is based on the assumption that such subpopulations persist stably over time, which could be examined through additional experiments, while an individual cell might produce both types of viral progeny in different proportions. In the *second scenario* (results in Section B the Supplementary Material), we consider one infected cell compartment. That compartment releases both mature and immature virions in a proportion $(1-\alpha)$ to α, and a fraction α of the infected cells contributes to additional interferon production by pDCs due to cell–cell contact.

Some results from the simulations in the *second scenario* are in qualitative agreement with those of the *first scenario* (statistical tests, shape of trade-offs, etc., refer to Figs. B.1–B.9 in the Supplementary Material). The sensitivities of model parameters (Figs. B.12–B.15 in the Supplementary Material) in the second scenario are not very similar to the first scenarios considered. This could be explained by the fact that the splitting/uniting of the infected cell compartment between the scenarios may lead to changes in the condition numbers of the respective system matrices. We conclude from these numerical experiments that further experimental work is necessary to elucidate and quantify the interactions in the immune response to mature and immature DENV, and the two scenarios considered in our work can be seen as first, simple steps in modelling mathematically this complex system.

Possible extensions of the model would be to include a continuum structure or trait of the DENV particles denoting the different levels of maturation and infectivity due to the degree of furin expression in the target cells and hence the degree of prM cleavage of the DENV particle (Pierson and Diamond 2012). Such approach is used in models of cancer, e.g. (Dimitriu et al. 2014). In addition, the parameter α may not necessarily remain constant over time, and time-series experiments could reveal whether the share of immature DENV changes over the course of the disease.

Yet, quantifying degrees of infectivity in an experimental in vivo setting, and understanding the interactions between virus and target cells may become highly complicated.

Furthermore, in the two scenarios considered here, we have omitted other kinds of antibody which could play a role in DENV viral dynamics (e.g. anti-E antibody) and other types of immune cells such as B cells or different subtypes of T cells. Evidence about ability of antibody to block the virion epitopes and threshold levels for neutralisation is inconclusive (Rodenhuis-Zybert et al. 2011), and may require modelling the functional response for NK cells, T cells, antibody not by a linear term as we have done, but with a Hill-type or a step function. Our model would be greatly supported by validation with experimental data and better approaches for quantifying potential heterogeneity among DENV-infected cells in expressing furin and its effect of synthesis of dengue virions with different maturities.

Our model could be a useful stepping stone for setting up new experiments both on cell and patient level. Efforts could be directed towards verifying the existence and persistence of distinct subpopulations of infected cells that produce mature versus immature virions and if these subpopulations persist, establish quantitatively differences in their dynamics. Immune indicators could be studied jointly with susceptibility to mosquito bites and the chances of viral transmission between patients and mosquito vectors. Additional data on the within-host dynamics of mature and immature virions could also be useful in clarifying the role of the different virions, as well as for analysing the effect of various preventive measures such as vaccines or mosquito repellents.

Acknowledgements This publication is based on work from COST Action CA16227 *Investigation & Mathematical Analysis of Avant-garde Disease Control via Mosquito Nano-Tech-Repellents*, supported by COST (European Cooperation in Science and Technology). Weblink: www.cost.eu. Peter Rashkov would like to thank the Mathematical Biosciences Institute (funded from the National Science Foundation Division of Mathematical Sciences and supported by The Ohio State University) for the opportunity to participate in the Emphasis Semester on Infectious Diseases: Data, Modelling, Decisions (Spring 2018). The authors thank Libin Rong and Nikolay I. Nikolov for the helpful discussions during the manuscript revision.

References

Anderson R, Wang S, Osiowy C, Issekutz AC (1997) Activation of endothelial cells via antibody-enhanced dengue virus infection of peripheral blood monocytes. J Virol 71(6):4226–4232

Ansari N, Hesaaraki M (2012) A within host dengue infection model with immune response and Beddington–DeAngelis incidence rate. Appl Math 3:177–184

Asselin-Paturel C, Brizard G, Chemin K, Boonstra A, O?Garra A, Vicari A, Trinchieri G (2005) Type I interferon dependence of plasmacytoid dendritic cell activation and migration. J Exp Med 201(7):1157–1167

Beltramello M, Williams KL, Simmons CP, Macagno A, Simonelli L, Quyen N, Sukupolvi-Petty S, Navarro-Sanchez E, Young PR, de Silva AM, Rey FA, Varani L, Whitehead SS, Diamond MS, Harris E, Lanzavecchia A, Sallusto F (2010) The human immune response to dengue virus is dominated by highly cross-reactive antibodies endowed with neutralizing and enhancing activity. Cell Host Microbe 8(3):271–283

Ben-Shachar R, Koelle K (2015) Minimal within-host dengue models highlight the specific roles of the immune response in primary and secondary dengue infections. J R Soc Interface 12:20140886

Ben-Shachar R, Schmidler S, Koelle K (2016) Drivers of inter-individual variation in dengue viral load dynamics. PLoS Comput Biol 12(11):e1005194

Bray M, Lai C (1991) Dengue virus premembrane and membrane proteins elicit a protective immune response. Virology 185(1):505–508

Chen X, Liu X, Liu W, Guo W, Yu Q, Wang C (2013) Comparative analysis of dendritic cell numbers and subsets between smoking and control subjects in the peripheral blood. Int J Clin Exp Patho 6(2):290–296

Clapham H, Tricou V, Van Vinh Chau N, Simmons C, Ferguson N (2014) Within-host viral dynamics of dengue serotype 1 infection. J R Soc Interface 11:20140094

Costa VV, Fagundes CT, Souza DG, Teixeira MM (2013) Inflammatory and innate immune responses in dengue infection: protection versus disease induction. Am J Pathol 182(6):1950–1961

Décembre E, Assil S, Hillaire MLB, Dejnirattisai W, Mongkolsapaya J, Screaton GR, Davidson AD, Dreux M (2014) Sensing of immature particles produced by dengue virus infected cells induces an antiviral response by plasmacytoid dendritic cells. PLoS Pathog 10(10):1004434

Dejnirattisai W, Jumnainsong A, Onsirisakul N, Fitton P, Vasanawathana S, Limpitikul W, Puttikhunt C, Edwards C, Duangchinda T, Supasa S, Chawansuntati K, Malasit P, Mongkolsapaya J, Screaton G (2010) Cross-reacting antibodies enhance dengue virus infection in humans. Science 328(5979):745–748

Dimitriu G, Lorenzi T, Ştefănescu R (2014) Evolutionary dynamics of cancer cell populations under immune selection pressure and optimal control of chemotherapy. Math Model Nat Phenom 9:88–104

van den Driessche P, Watmough J (2002) Reproduction numbers and sub-threshold endemic equilibria for compartmental models of disease transmission. Math Biosci 180:29–48

Dung NTP, Duyen HTL, Thuy NTV, Ngoc TV, Chau NVV, Hien TT, Rowland-Jones SL, Dong T, Farrar J, Wills B, Simmons CP (2010) Timing of CD8+ T cell responses in relation to commencement of capillary leakage in children with dengue. J Immunol 184(12):7281–7287

Duong V, Lambrechts L, Paul RE, Ly S, Lay RS, Long KC, Huy R, Tarantola A, Scott TW, Sakuntabhai A, Buchya P (2015) Asymptomatic humans transmit dengue virus to mosquitoes. Proc Natl Acad Sci USA 11:14688–14693

Fitzgerald-Bocarsly P, Dai J, Singh S (2008) Plasmacytoid dendritic cells and type I IFN: 50 years of convergent history. Cytokine Growth F R 19(1):3–19

Friberg H, Bashyam H, Toyosaki-Maeda T, Potts J, Greenough T, Kalayanarooj S, Gibbons R, Nisalak A, Srikiatkhachorn A, Green S, Stephens H, Rothman A, Mathew A (2011) Cross-reactivity and expansion of dengue-specific t cells during acute primary and secondary infections in humans. Sci Rep 1:51

Gibbons JD, Chakraborti S (2010) Nonparametric statistical inference, 5th edn. Taylor and Francis, Boca Raton, FL

Green S, Pichyangkul S, Vaughn DW, Kalayanarooj S, Nimmannitya S, Nisalak A, Kurane I, Rothman AL, Ennis FA (1999) Early cd69 expression on peripheral blood lymphocytes from children with dengue hemorrhagic fever. J Infect Dis 180(5):1429–1435

Gujarati T, Ambika G (2014) Virus antibody dynamics in primary and secondary dengue infections. J Math Biol 69:1773–1800

Halstead S, O'Rourke E (1977) Antibody-enhanced dengue virus infection in primate leukocytes. Nature 265(5596):739–741

Heinz FX, Stiasny K, Pschner-Auer G, Holzmann H, Allison SL, Mandl CW, Kunz C (1994) Structural changes and functional control of the tick-borne encephalitis virus glycoprotein e by the heterodimeric association with protein prm. Virology 198(1):109–117

Kurane I, Rothman AL, Livingston PG, Green S, Gagnon SJ, Janus J, Innis BL, Nimmannitya S, Nisalak A, Ennis FA (1994) Immunopathologic mechanisms of dengue hemorrhagic fever and dengue shock syndrome. In: Brinton MA, Calisher CH, Rueckert R (eds) Positive-strand RNA viruses, pp 59–64. Springer, Vienna

Marino S, Hogue IB, Ray CJ, Kirschner DE (2008) A methodology for performing global uncertainty and sensitivity analysis in systems biology. J Theor Biol 254(1):178–196

Mathan T, Figdor C, Buschow S (2013) Human plasmacytoid dendritic cells: from molecules to intercellular communication network. Front Immunol 4:372

Mathew A, Rothman AL (2008) Understanding the contribution of cellular immunity to dengue disease pathogenesis. Immunol Rev 225(1):300–313

McKenna K, Beignon AS, Bhardwaj N (2005) Plasmacytoid dendritic cells: linking innate and adaptive immunity. J Virol 79(1):17–27
Montoya M, Schiavoni G, Mattei F, Gresser I, Belardelli F, Borrow P, Tough DF (2002) Type i interferons produced by dendritic cells promote their phenotypic and functional activation. Blood 99(9):3263–3271
Nikin-Beers R, Ciupe SM (2015) The role of antibody in enhancing dengue virus infection. Math Biosci 263:83–92
Nuraini N, Tasman H, Soewono E, Sidarto KA (2009) A with-in host dengue infection model with immune response. Math Comput Model 49(5):1148–1155
Pichyangkul S, Endy TP, Kalayanarooj S, Nisalak A, Yongvanitchit K, Green S, Rothman AL, Ennis FA, Libraty DH (2003) A blunted blood plasmacytoid dendritic cell response to an acute systemic viral infection is associated with increased disease severity. J Immunol 171(10):5571–5578
Pierson TC, Diamond MS (2012) Degrees of maturity: the complex structure and biology of flaviviruses. Curr Opin Virol 2(2):168–175
Rodenhuis-Zybert IA, van der Schaar HM, da Silva Voorham JM, van der Ende-Metselaar H, Lei HY, Wilschut J, Smit JM (2010) Immature dengue virus: a veiled pathogen? PLoS Pathog 6(1):1000718
Rodenhuis-Zybert IA, Wilschut J, Smit JM (2011) Partial maturation: an immune-evasion strategy of dengue virus? Trends Microbiol 19(5):248–254
Silveira GF, Wowk PF, Cataneo AHD, dos Santos PF, Delgobo M, Stimamiglio MA, Lo Sarzi M, Thomazelli APFS, Conchon-Costa I, Pavanelli WR, Antonelli LRV, Báfica A, Mansur DS, dos Santos CND, Bordignon J (2018) Human T lymphocytes are permissive for dengue virus replication. J Virol 92(10):e02181
Tough D (2012) Modulation of T-cell function by type I interferon. Immunol Cell Biol 90:492–497
Waggoner JJ, Balmaseda A, Gresh L, Sahoo MK, Montoya M, Wang C, Abeynayake J, Kuan G, Pinsky BA, Harris E (2016) Homotypic dengue virus reinfections in Nicaraguan children. J Infect Dis 214(7):986–993
Wang S, Wang X, Liu M, Bai O (2018) Blastic plasmacytoid dendritic cell neoplasm: update on therapy especially novel agents. Ann Hematol 97:563–572
Webster B, Werneke SW, Zafirova B, This S, Coléon S, Décembre E, Paidassi H, Bouvier I, Joubert PE, Duffy D, Walzer T, Albert ML, Dreux M (2018) Plasmacytoid dendritic cells control dengue and chikungunya virus infections via IRF7-regulated interferon responses. eLife 7:e34273
Zybert IA, van der Ende-Metselaar H, Wilschut J, Smit JM (2008) Functional importance of dengue virus maturation: infectious properties of immature virions. J Gen Virol 89(12):3047–3051

Affiliations

Milen Borisov[1] · Gabriel Dimitriu[2] · Peter Rashkov[1]

Gabriel Dimitriu
gabriel.dimitriu@umfiasi.ro

[1] Institute of Mathematics and Informatics, Bulgarian Academy of Sciences, 1113 Sofia, Bulgaria

[2] University of Medicine and Pharmacy "Grigore T. Popa", Universitatii 16, Iaşi, Romania